

Effective field theory of ${}^3\text{He}$

S.-I. Ando^a

Department of Physics Education, Daegu University, Gyeongsan 712-714, Republic of Korea

Abstract. We report the results of our recent calculations of three nucleon bound states, ${}^3\text{H}$ and ${}^3\text{He}$, in pionless effective field theory including di-baryon fields at leading order, treating the Coulomb interaction nonperturbatively.

1 Introduction

In the limit where two-body scattering length a_2 (two-body binding energy B_2) goes to infinity (nil), infinitely many three-body bound states are accumulated at the three-body scattering threshold with a geometric spectrum. Those states are known as Efimov states [1]. Because the S-wave two nucleon scattering length is very large, $a_{np} = -23.7$ fm, and two nucleon binding energy (deuteron binding energy) is very small, $B_2 = 2.22$ MeV, even compared to the chiral symmetry breaking scale, *i.e.*, the pion mass, $m_\pi = 140$ MeV, three-nucleon bound states, tritium and ${}^3\text{He}$, could be considered as Efimov states.

The pionless effective field theory (EFT) including di-baryon fields has been applied to the study of spin doublet nd scattering and tritium [2]. (For a recent review, see, e.g., Ref. [3].) In the renormalization group (RG) analysis in that study, an oscillating behavior of the scattering amplitude in UV limit of a cutoff parameter is observed, and in order to make the amplitude cutoff independence, a nucleon-nucleon-di-baryon-di-baryon contact interaction is promoted to the leading order, which appears as a higher order term in the naive dimensional analysis. In other words, the contact three-body interaction exhibits the oscillating behavior, so called limit-cycle, and the oscillating pattern of the three-body contact term corresponds to the geometric spectrum of the Efimov states.

The ${}^3\text{He}$ nucleus is of particular interest since it can potentially provide access to properties of the neutron that require a polarized target. It should be possible to describe its low-energy properties within the pionless EFT, extended to include the Coulomb interaction. However the only previous application of the theory to the pd system is in the work of Rupak and Kong, who treated Coulomb effects perturbatively and only considered the spin-3/2 channel [4]. (Recently, this approach is extended to the pd channel in spin 1/2 and ${}^3\text{He}$ channel[5].) Also, it is needed to answer the question of whether the Efimov effect survives in the presence of the Coulomb interaction. Arguments based on the degrees of the singularities in the potentials suggest it should and this has been checked by Hammer and Higa for a simpler two-body model [6]. However it has not previously been confirmed in a three-body system.

Here we report the results of a study of ${}^3\text{He}$ in the pionless EFT with the Coulomb interaction treated nonperturbatively [7]. Our approach is based on that used by Kok *et al.* [8] to study ${}^3\text{He}$ with separable potentials and the full off-shell Coulomb T -matrix. Our results show that the Efimov effect does indeed occur in the presence of the Coulomb interaction. We also determine the strength of the three-body force needed to reproduce observed ${}^3\text{He}$ binding energy. The difference between this and the corresponding force needed for the triton is of the expected size for an electromagnetic effect.

^a e-mail: sando@daegu.ac.kr

2 Lagrangian

The effective Lagrangian for the three-nucleon system can be written as [2,9]

$$\mathcal{L} = \mathcal{L}_N + \mathcal{L}_s + \mathcal{L}_t + \mathcal{L}_3, \quad (1)$$

where \mathcal{L}_N is the standard one-nucleon Lagrangian in the heavy-baryon formalism,

$$\mathcal{L}_N = N^\dagger \left\{ iv \cdot D + \frac{1}{2m_N} [(v \cdot D)^2 - D^2] \right\} N. \quad (2)$$

Here v^μ is a velocity vector satisfying a condition $v^2 = 1$, D_μ is the covariant derivative, and m_N is the nucleon mass. The terms \mathcal{L}_s and \mathcal{L}_t are di-baryon effective Lagrangian for spin singlet and triplet parts, respectively, and these read

$$\mathcal{L}_s = \sigma_s s_a^\dagger \left\{ iv \cdot D + \frac{1}{4m_N} [(v \cdot D)^2 - D^2] + \Delta_{s(a)} \right\} s_a - y_s \left\{ s_a^\dagger [N^T P_a^{(1S_0)} N] + h.c. \right\}, \quad (3)$$

$$\mathcal{L}_t = \sigma_t t_i^\dagger \left\{ iv \cdot D + \frac{1}{4m_N} [(v \cdot D)^2 - D^2] + \Delta_t \right\} t_i - y_t \left\{ t_i^\dagger [N^T P_i^{(3S_1)} N] + h.c. \right\}, \quad (4)$$

where s_a and t_i are the corresponding di-baryon fields. $\sigma_{s,t}$ is a sign factor, $\sigma_{s,t} = -1$. The strengths of the corresponding two-body interactions depend on $\Delta_{s(a)}$ and Δ_t , the mass differences between the di-baryons and two nucleons, and y_s and y_t , the coupling constants for the di-baryon-nucleon-nucleon vertices. The projection operators for the two-nucleon 1S_0 and 3S_1 states are

$$P_a^{(1S_0)} = \frac{1}{\sqrt{8}} \tau_2 \tau_a \sigma_2, \quad P_i^{(3S_1)} = \frac{1}{\sqrt{8}} \tau_2 \sigma_2 \sigma_i, \quad (5)$$

where τ_a and σ_i are Pauli matrices for isospin and spin, respectively.

The three-body force is expressed as a di-baryon-nucleon contact interaction. It is given by the effective Lagrangian,

$$\mathcal{L}_3 = \frac{m_N H(\Lambda)}{3\Lambda^2} \left\{ y_t^2 N^\dagger (\sigma \cdot \mathbf{t})^\dagger (\sigma \cdot \mathbf{t}) N - y_s y_t [N^\dagger (\sigma \cdot \mathbf{t})^\dagger (\tau \cdot \mathbf{s}) N + h.c.] + y_s^2 N^\dagger (\tau \cdot \mathbf{s})^\dagger (\tau \cdot \mathbf{s}) N \right\}, \quad (6)$$

where $H(\Lambda)$ is the coupling constant, which runs with the scale Λ of the cutoff we impose on the coupled integral equations. Note that this interaction contributes only to three-body channels with total spin 1/2 and total isospin 1/2.

The building blocks needed to construct the three-body integral equations from the Lagrangian are as follows. In the one-body sector, we have the non-relativistic nucleon propagator,

$$iS_N(p) = \frac{i}{p_0 - \frac{\mathbf{p}^2}{2m_N} + i\epsilon}. \quad (7)$$

In the two-body sector, we need the dressed di-baryon propagators with and without the Coulomb interaction. The propagators for the np and nm channels, which have no Coulomb interaction, are



Fig. 1. Diagrams for the dressed di-baryon propagator, denoted by the double line with filled circle. Single lines represent nucleon propagators; double lines undressed di-baryon propagators.

represented by the diagrams in Fig. 1 and are given by

$$iD_{s,t} \left(E - \frac{3q^2}{4m_N} \right) = \frac{4\pi}{m_N y_{s,t}^2} \frac{-i}{-\mu - \frac{4\pi\Delta_{s,t}}{m_N y_{s,t}^2} + \sqrt{\frac{3}{4}q^2 - m_N E - i\epsilon + i\epsilon}}. \quad (8)$$

The two-nucleon loop diagrams here have been dimensionally regularized using the PDS scheme with the subtraction scale μ . The dependence on this can be removed by renormalizing the constants $4\pi\Delta_{s,t}/(m_N y_{s,t}^2)$ using

$$\mu + \frac{4\pi\Delta_{s(np)}}{m_N y_s^2} = \frac{1}{a_{np}}, \quad \mu + \frac{4\pi\Delta_{s(nn)}}{m_N y_s^2} = \frac{1}{a_{nn}}, \quad \mu + \frac{4\pi\Delta_t}{m_N y_t^2} = \gamma, \quad (9)$$

where a_{np} and a_{nn} are the scattering lengths for the spin-singlet np and nn channels, respectively, and γ is related to the deuteron binding energy B_2 through $\gamma = \sqrt{m_N B_2}$. Working to leading order, we neglect corrections from the effective ranges.

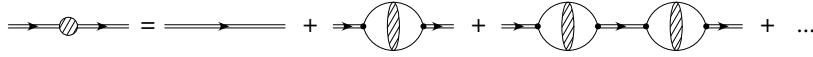


Fig. 2. Diagrams for dressed dibaryon propagator for the pp channel, denoted by the double line with shaded circle. The shaded ovals here represent the two-nucleon Green's function dressed with the Coulomb interaction.

In the pp channel, the Coulomb interaction dresses the two-nucleon Green's function in the bubble diagram for the dressed di-baryon propagator, as shown in Fig. 2. The resulting propagator is given by

$$iD_{s(pp)} \left(E - \frac{3q^2}{4m_N} \right) = \frac{4\pi}{m_N y_s^2} \frac{-i}{-\frac{4\pi\Delta_{s(pp)}^R}{m y_s^2} - 2\kappa H(\kappa/p')}, \quad (10)$$

where

$$H(\eta) = \psi(i\eta) + \frac{1}{2i\eta} - \ln(i\eta), \quad (11)$$

ψ is the logarithmic derivative of the Γ function, and $-ip' = \sqrt{\frac{3}{4}q^2 - m_N E - i\epsilon}$. The renormalized constant $\Delta_{s(pp)}^R$ for the pp channel cancels both the linear and logarithmic divergences of the loop diagram. It is related to the Coulomb scattering length a_C by

$$\frac{1}{a_C} = \frac{4\pi\Delta_{s(pp)}^R}{m_N y_s^2} = \frac{4\pi\Delta_{s(pp)}}{m_N y_s^2} + \mu - 2\kappa \left[1 - C_E + \ln\left(\frac{\mu}{4\kappa}\right) \right], \quad (12)$$

where $C_E = 0.577215\dots$ is Euler's constant. Note that the logarithmic divergence means that it is impossible to make a model-independent decomposition of $1/a_C$ into strong and electromagnetic contributions [10–12]. This implies that within this EFT there is no unambiguous way to separate Coulomb from other isospin-breaking effects.

The final building block for the integral equations is the off-shell Coulomb T-matrix. A convenient form for it is the integral representation [13] for negative energies, $k^2/m_N < 0$:

$$\langle \mathbf{p}' | T_C(k^2/m_N) | \mathbf{p} \rangle = \frac{e^2}{(\mathbf{p}' - \mathbf{p})^2} \left[1 - 4i\eta \int_0^1 dt \frac{t^\eta}{4t - (1-t)^2(x^2 - 1)} \right], \quad (13)$$

where $\eta = \kappa/k$ and

$$x^2 = 1 + \frac{(p'^2 - k^2)(p^2 - k^2)}{k^2(\mathbf{p}' - \mathbf{p})^2}. \quad (14)$$

3 Integral equations

Now we construct the integral equations for scattering of a third nucleon off a deuteron, concentrating on the channels where the third nucleon is in an S wave, and the total spin and isospin of the three particles are both $1/2$. The negative-energy solutions of these describe the bound triton and ${}^3\text{He}$ states.

We work the center of mass frame for the Nd scattering and use the notation of Bedaque *et al.* [2]. In the isospin-symmetric case, this process can be described by an amplitude $a(p, k)$ for scattering into states with a 3S_1 di-baryon, and $b(p, k)$ for scattering into those with a 1S_0 di-baryon. Here k denotes the initial (on-shell) relative momentum of the deuteron and the third nucleon, and p the final (off-shell) momentum. The amplitudes satisfy coupled integral equations which can be represented diagrammatically as in Fig. 3. The kernels of these equations consist of two terms: one-nucleon-exchange, which provides a long-range force between the di-baryon and the third nucleon, and the three-body contact interaction.

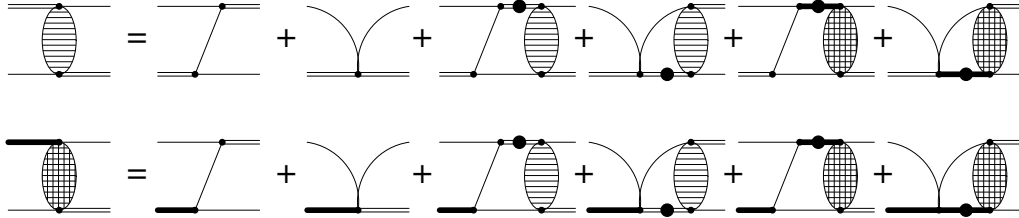


Fig. 3. Diagrams corresponding to the coupled integral equations for nucleon-di-baryon scattering. Thin lines denote nucleons, double and thick lines 3S_1 and 1S_0 di-baryons. Those with filled circles are dressed di-baryon propagators, as in Fig. 1. Ovals with stripes denote the off-shell amplitude $a(p, k)$ with initial and final spin-triplet di-baryons, and those with cross stripes the amplitude $b(p, k)$ with initial spin-triplet and final spin-singlet di-baryon fields.

When we include the Coulomb interaction, isospin symmetry is broken and we must introduce separate amplitudes $b_+(p, k)$ and $b_0(p, k)$ for pd scattering into states with 1S_0 pp and np di-baryons, respectively. These and $a(p, k)$ satisfy a set of three coupled integral equations. For completeness, we also present the corresponding set of three equations that arise when we allow for isospin-breaking effects in the nd case, involving the amplitude $b_-(p, k)$ for states with nm di-baryons.

3.1 Integral equations for the nd channel

Before presenting the equations for pd scattering, we first look at the simpler equations for nd scattering. Allowing for isospin breaking in the scattering lengths, the three integral equations for the $S = 1/2, T = 1/2$ channel are

$$\begin{aligned}
 a(p, k) = & K^{(a)}(p, k; E) + 2 \frac{H(\Lambda)}{\Lambda^2} \\
 & + \frac{1}{\pi} \int_0^\Lambda dq q^2 \left[K^{(a)}(p, q; E) + 2 \frac{H(\Lambda)}{\Lambda^2} \right] \frac{a(q, k)}{-\gamma + \sqrt{\frac{3}{4}q^2 - mE}} \\
 & + \frac{1}{\pi} \int_0^\Lambda dq q^2 \left[K^{(a)}(p, q; E) + \frac{2}{3} \frac{H(\Lambda)}{\Lambda^2} \right] \frac{b_0(q, k)}{-\frac{1}{a_{np}} + \sqrt{\frac{3}{4}q^2 - mE}} \\
 & + \frac{2}{\pi} \int_0^\Lambda dq q^2 \left[K^{(a)}(p, q; E) + \frac{2}{3} \frac{H(\Lambda)}{\Lambda^2} \right] \frac{b_-(q, k)}{-\frac{1}{a_{nn}} + \sqrt{\frac{3}{4}q^2 - mE}}, \quad (15)
 \end{aligned}$$

$$\begin{aligned}
 b_0(p, k) &= 3K^{(a)}(p, k; E) + 2 \frac{H(\Lambda)}{\Lambda^2} \\
 &+ \frac{1}{\pi} \int_0^\Lambda dq q^2 \left[3K^{(a)}(p, q; E) + 2 \frac{H(\Lambda)}{\Lambda^2} \right] \frac{a(q, k)}{-\gamma + \sqrt{\frac{3}{4}q^2 - mE}} \\
 &+ \frac{1}{\pi} \int_0^\Lambda dq q^2 \left[-K^{(a)}(p, q; E) + \frac{2}{3} \frac{H(\Lambda)}{\Lambda^2} \right] \frac{b_0(q, k)}{-\frac{1}{a_{np}} + \sqrt{\frac{3}{4}q^2 - mE}} \\
 &+ \frac{2}{\pi} \int_0^\Lambda dq q^2 \left[K^{(a)}(p, q; E) + \frac{2}{3} \frac{H(\Lambda)}{\Lambda^2} \right] \frac{b_-(q, k)}{-\frac{1}{a_{nn}} + \sqrt{\frac{3}{4}q^2 - mE}}, \quad (16)
 \end{aligned}$$

$$\begin{aligned}
 b_-(p, k) &= 3K^{(a)}(p, k; E) + 2 \frac{H(\Lambda)}{\Lambda^2} \\
 &+ \frac{1}{\pi} \int_0^\Lambda dq q^2 \left[3K^{(a)}(p, q; E) + 2 \frac{H(\Lambda)}{\Lambda^2} \right] \frac{a(q, k)}{-\gamma + \sqrt{\frac{3}{4}q^2 - mE}} \\
 &+ \frac{1}{\pi} \int_0^\Lambda dq q^2 \left[K^{(a)}(p, q; E) + \frac{2}{3} \frac{H(\Lambda)}{\Lambda^2} \right] \frac{b_0(q, k)}{-\frac{1}{a_{np}} + \sqrt{\frac{3}{4}q^2 - mE}} \\
 &+ \frac{2}{\pi} \int_0^\Lambda dq q^2 \left[\frac{2}{3} \frac{H(\Lambda)}{\Lambda^2} \right] \frac{b_-(q, k)}{-\frac{1}{a_{nn}} + \sqrt{\frac{3}{4}q^2 - mE}}, \quad (17)
 \end{aligned}$$

where

$$K^{(a)}(p, q; E) = \frac{1}{2pq} \ln \left(\frac{p^2 + q^2 + 2pq - m_N E}{p^2 + q^2 - 2pq - m_N E} \right). \quad (18)$$

If we set $a_{nn} = a_{np}$ and $b_0 = b_- = b$, these reduce to the isospin-symmetric forms of the equations in Ref. [2]. The integrals over the relative momentum q are all cut off at $q = \Lambda$. The resulting dependence on Λ can be cancelled by the three-body force, whose strength is $H(\Lambda)/\Lambda^2$.

3.2 Integral equations for the pd channel

We now turn to the corresponding equations for pd scattering. These differ from the ones in the previous subsection by having b_+ instead of b_- and, more importantly, adding the Coulomb interaction between the two protons. They can be obtained from the equations developed by the Groningen group [8], by omitting the separable form factors and instead imposing a sharp cutoff on the relative momenta.

The Coulomb interaction leads to additional long-range terms in the kernels of these equations. The diagrams for the full long-range kernel are shown in Fig. 4. The one-nucleon exchange term of diagram (a) is supplemented by diagram (b) if a proton is exchanged, and by (c) for neutron exchange. Finally, diagram (d) represents the Coulomb interaction between an np di-baryon and a proton.

The coupled integral equations can be written

$$\begin{aligned}
 a(p, k) &= K^{(a)}(p, k; E) + K^{(c)}(p, k; E) + 2K^{(d)}(p, k; E) + 2 \frac{H(\Lambda)}{\Lambda^2} \\
 &+ \frac{1}{\pi} \int_0^\Lambda dq q^2 \left[K^{(a)}(p, q; E) + K^{(c)}(p, q; E) + 2K^{(d)}(p, q; E) + 2 \frac{H(\Lambda)}{\Lambda^2} \right] \\
 &\quad \times \frac{a(q, k)}{-\gamma + \sqrt{\frac{3}{4}q^2 - mE}}
 \end{aligned}$$

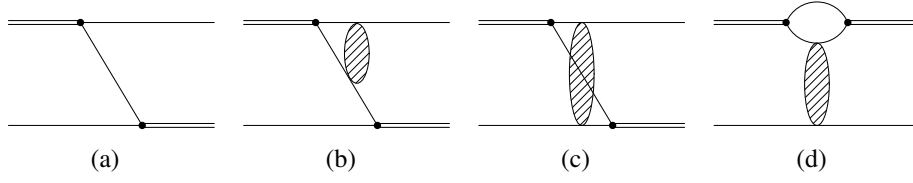


Fig. 4. Diagrams corresponding to the long-range terms in the kernel for pd scattering. Here, the shaded oval denotes the off-shell Coulomb T -matrix (since contributions where the two protons do not interact are already contained in (a)). Diagram (b) has been shown for the case of an initial np di-baryon and a final pp one. The corresponding diagram for the inverse process is the mirror image of this.

$$\begin{aligned}
 & + \frac{1}{\pi} \int_0^\Lambda dq q^2 \left[K^{(a)}(p, q; E) + K^{(c)}(p, k; E) + \frac{2}{3} \frac{H(\Lambda)}{\Lambda^2} \right] \frac{b_0(q, k)}{-\frac{1}{a_{np}} + \sqrt{\frac{3}{4}q^2 - mE}} \\
 & + \frac{2}{\pi} \int_0^\Lambda dq q^2 \left[K^{(a)}(p, k; E) + K_{13}^{(b)}(p, k; E) + \frac{2}{3} \frac{H(\Lambda)}{\Lambda^2} \right] \frac{b_+(q, k)}{-\frac{1}{a_c} - 2\kappa H(\kappa/p')},
 \end{aligned} \tag{19}$$

$$\begin{aligned}
 b_0(p, k) &= 3K^{(a)}(p, k; E) + 3K^{(c)}(p, k; E) + 2 \frac{H(\Lambda)}{\Lambda^2} \\
 & + \frac{1}{\pi} \int_0^\Lambda dq q^2 \left[3K^{(a)}(p, q; E) + 3K^{(c)}(p, q; E) + 2 \frac{H(\Lambda)}{\Lambda^2} \right] \frac{a(q, k)}{-\gamma + \sqrt{\frac{3}{4}q^2 - mE}} \\
 & - \frac{1}{\pi} \int_0^\Lambda dq q^2 \left[K^{(a)}(p, q; E) + K^{(c)}(p, q; E) + 2K^{(d)}(p, q; E) - \frac{2}{3} \frac{H(\Lambda)}{\Lambda^2} \right] \\
 & \quad \times \frac{b_0(q, k)}{-\frac{1}{a_{np}} + \sqrt{\frac{3}{4}q^2 - mE}} \\
 & + \frac{2}{\pi} \int_0^\Lambda dq q^2 \left[K^{(a)}(p, q; E) + K_{13}^{(b)}(p, q; E) + \frac{2}{3} \frac{H(\Lambda)}{\Lambda^2} \right] \frac{b_+(q, k)}{-\frac{1}{a_c} - 2\kappa H(\kappa/p')},
 \end{aligned} \tag{20}$$

$$\begin{aligned}
 b_+(p, k) &= 3K^{(a)}(p, k; E) + 3K_{31}^{(b)}(p, k; E) + 2 \frac{H(\Lambda)}{\Lambda^2} \\
 & + \frac{1}{\pi} \int_0^\Lambda dq q^2 \left[3K^{(a)}(p, q; E) + 3K_{31}^{(b)}(p, q; E) + 2 \frac{H(\Lambda)}{\Lambda^2} \right] \frac{a(q, k)}{-\gamma + \sqrt{\frac{3}{4}q^2 - mE}} \\
 & + \frac{1}{\pi} \int_0^\Lambda dq q^2 \left[K^{(a)}(p, k; E) + K_{31}^{(b)}(p, q; E) + \frac{2}{3} \frac{H(\Lambda)}{\Lambda^2} \right] \frac{b_0(q, k)}{-\frac{1}{a_{np}} + \sqrt{\frac{3}{4}q^2 - mE}} \\
 & + \frac{2}{\pi} \int_0^\Lambda dq q^2 \left[\frac{2}{3} \frac{H(\Lambda)}{\Lambda^2} \right] \frac{b_+(q, k)}{-\frac{1}{a_c} - 2\kappa H(\kappa/p')},
 \end{aligned} \tag{21}$$

where $K^{(a)}$ is the one-nucleon exchange kernel defined in Eq. (18) above, and $K_{31}^{(b)}$, $K_{13}^{(b)}$, $K^{(c)}$, and $K^{(d)}$ are the pieces corresponding to the Coulomb diagrams (b), (c), (d) in Fig. 4. (In $K_{31}^{(b)}$ and $K_{13}^{(b)}$, the subscripts 1 and 3 refer to initial and final di-baryons, 1 denoting np and 3 pp .) Explicit expressions of the kernels can be found in Ref. [7].

4 Numerical results for bound states

We solve for the three-body bound states by taking the homogeneous parts of the coupled integral equations and treating them as nonlinear eigenvalue problems,

$$K(E)u = u, \quad (22)$$

where $u^T = (a, b_0, b_{\pm})$ and the 3×3 matrices of integral operators $K(E)$ can be extracted from the expressions in the previous section. Detailed explanation for the numerical calculation is referred to Ref. [7].

For given values of the two-body input parameters we first set the three-body force $H(\Lambda)$ to zero and adjust the value of the cutoff until the shallowest bound-state eigenvalue reproduces the observed three-body binding energy. Starting from this cutoff, Λ_0 , we then determine the values of $H(\Lambda)$ needed to reproduce this binding energy for other cutoffs.

4.1 Triton

In this case, we work with the determinant constructed from the homogeneous part of the coupled integral equations in Eqs. (15), (16), and (17). The two-body input is provided by

$$\gamma = 45.703 \text{ MeV}, \quad a_{np} = -23.749 \pm 0.008 \text{ fm [14]}, \quad a_{nn} = -18.5 \pm 0.4 \text{ fm [15]}. \quad (23)$$

We adjust the three-body force to fit the triton binding energy,

$$B_3(^3\text{H}) = 8.48182 \text{ MeV}, \quad (24)$$

which corresponds to a momentum scale $\alpha = \sqrt{m_N B_3} = 89.239 \text{ MeV}$.

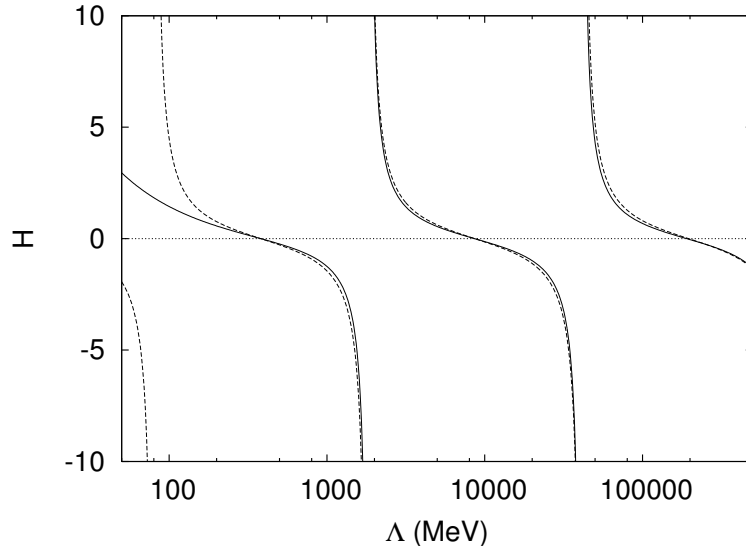


Fig. 5. Values of the three-body force H as a function of the cutoff Λ in MeV. For comparison, the dashed curve shows the asymptotic, scale-free form of $H(\Lambda)$.

For $H(\Lambda) = 0$, we reproduce the experimental binding energy with the cutoff $\Lambda_0 = 380.689 \text{ MeV}$. The values of the three-body force needed for other cutoffs are shown in Fig. 5.

As we take $\Lambda \rightarrow \infty$, the cutoff becomes much larger than the physical scales in the system and $H(\Lambda)$ displays the limit-cycle behavior found in Ref. [2]. This reflects the presence of the Efimov effect in this three-body system, a tower of deeply bound states with energies in a constant ratio [1]. In three-nucleon systems only the shallowest of these states lies within the domain of the EFT and so corresponds to a physical state.

The asymptotic form of $H(\Lambda)$ in this limit is [2]

$$H(\Lambda) = -\frac{\sin[s_0 \ln(\Lambda/\Lambda_*) - \arctan(1/s_0)]}{\sin[s_0 \ln(\Lambda/\Lambda_*) + \arctan(1/s_0)]}. \quad (25)$$

where $s_0 = 1.00624 \dots$ and the scale parameter Λ_* is defined by

$$\Lambda_0 = \Lambda_* \exp[(1/s_0) \arctan(1/s_0)]. \quad (26)$$

This form is shown by the dashed line in Fig. 5. The numerical results deviate from it only for small values of Λ where the finite scale can influence the renormalization of the three-body force.

4.2 ${}^3\text{He}$ channel

For the ${}^3\text{He}$ channel, we need to the pp Coulomb scattering length as a two-body input parameter,

$$a_C = -7.8063 \pm 0.0026 \text{ fm} [16]. \quad (27)$$

The experimental binding energy of ${}^3\text{He}$ is

$$B_3({}^3\text{He}) = 7.71804 \text{ MeV}, \quad (28)$$

corresponding to a scale $\alpha = 85.127 \text{ MeV}$

Firstly, assuming the isospin symmetry in the three-body contact interaction and using the Λ_0 value fixed by tritium binding energy above, we get $\alpha = 84.8084 \text{ MeV}$, or a binding energy of $B_3 = 7.66038 \text{ MeV}$ for ${}^3\text{He}$. This differs from the triton energy for the same three-body force by 0.82 MeV . It is within 1% of the observed ${}^3\text{He}$ energy, indicating that the isospin-violating three-body force is indeed a higher-order contribution. This is as expected, given the absence of any modification of the renormalization, since the isospin-violating term is suppressed by one power of the inverse Bohr radius κ relative to the LO force.

By adjusting the strength of the three-body force, we can fit the experimental binding energy. As in the triton case, we have done this for a range of cutoffs, and obtain $\Lambda_0 = 382.46 \text{ MeV}$. The results are plotted in Fig. 6. They display the same limit-cycle behavior as in the triton channel. Moreover the differences between the forces needed in the two channels are very small, reflecting the fact that a symmetric force can give a very good account of ${}^3\text{He}$.

5 Summary

We have studied ${}^3\text{He}$ within the framework of the pionless EFT, treating the Coulomb interaction nonperturbatively. We solve the set of integral equations developed by Kok *et al.* [8], which can be thought of as extending the equation of Skornyakov and ter-Martirosian [17] to include the full off-shell Coulomb T -matrix.

We find that a three-body interaction is required at leading order in ${}^3\text{He}$, as in the triton. This force also exhibits the same limit-cycle behavior as a function of the cutoff Λ as found by Bedaque *et al.* [2] for systems with purely short-range interactions. These results show that the Coulomb interaction is not singular enough to alter the deeply bound ‘‘Efimov’’ states in the three-nucleon system.

We find that an isospin symmetric three-body force, fit to the triton binding energy, can give the ${}^3\text{He}$ binding to better than 1%. The scale parameter of the force that fits ${}^3\text{He}$ differs from the corresponding value for the triton by about 0.5%. This is of the expected size for an order- α electromagnetic effect. Our results demonstrate that the Coulomb interaction has no nonperturbative effect on the renormalization of the three-body force in ${}^3\text{He}$. Moreover the overall contributions of the Coulomb interaction to the binding energy of ${}^3\text{He}$ are small, perhaps unsurprisingly given the typical momenta involved, and so could have been calculated perturbatively.

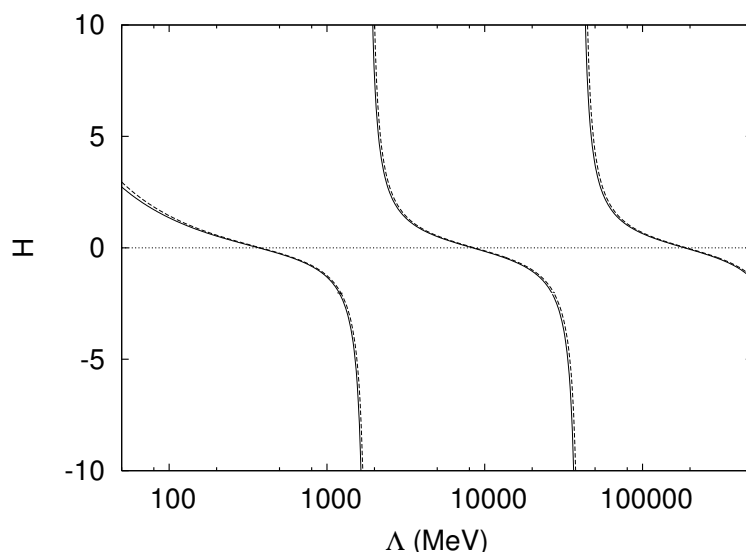


Fig. 6. Evolution with Λ of the three-body forces $H(\Lambda)$ for ${}^3\text{He}$ (solid line) and the triton (dashed).

Acknowledgments

The author thanks organizers of the workshop, HNP2011, for support and hospitality. The original work [7] has been done when he was in Manchester. He would like to thank Mike C. Birse for collaboration and stimulus discussions. The work was supported by STFC grants PP/F000448/1 and ST/F012047/1. He also thanks to Yupeng Yan for support and hospitality during his stay in Suranaree University of Technology when the manuscript is completed. This work was supported by Basic Science Research Program through the National Research Foundation of Korea (NRF) funded by the Ministry of Education, Science, and Technology (2010-0023661).

References

1. V. N. Efimov, *Sov. J. Nucl. Phys.* **12** (1971) 589; **76** (1979) 546.
2. P. F. Bedaque, H.-W. Hammer and U. van Kolck, *Nucl. Phys. A* **676**, 357 (2000).
3. H.-W. Hammer and L. Platter, *Ann. Rev. Nucl. Part. Sci.* **60** (2010) 207.
4. G. Rupak and X. Kong, *Nucl. Phys.* **A717**, 73 (2003).
5. S. König and H.-W. Hammer, arXiv:1101.5939.
6. H.-W. Hammer and R. Higa, *Eur. Phys. J.* **A37**, 193 (2008).
7. S. Ando and B. C. Birse, *J. Phys. G: Nucl. Part. Phys.* **37**, 105108 (2010).
8. L. P. Kok, D. J. Struik, and H. van Haeringen, University of Groningen Internal Report 151 (1975); L. P. Kok, D. J. Struik, J. E. Holwerda and H. van Haeringen, University of Groningen Internal Report 170 (1975).
9. S. Ando and C. H. Hyun, *Phys. Rev. C* **72**, 014008 (2005).
10. X. Kong and F. Ravndal, *Phys. Lett.* **B450**, 320 (1999); *Phys. Rev. C* **64**, 044002 (2001).
11. T. Barford and M. C. Birse, *Phys. Rev. C* **67**, 064006 (2003).
12. S. Ando, J. W. Shin, C. H. Hyun and S.-W. Hong, *Phys. Rev. C* **76**, 064001 (2007).
13. J. C. Y. Chen and A. C. Chen, *Adv. Atom. Mol. Phys.* **8**, 71 (1972).
14. L. Koester and W. Nistler, *Z. Phys. A* **272**, 189 (1975).
15. G. F. de Téramond and B. Gabioud, *Phys. Rev. C* **36**, 691 (1987).
16. J. R. Bergervoet, P. C. van Campen, T. A. Rijken and J. J. de Swart, *Phys. Rev. C* **38**, 770 (1988).
17. G. V. Skorniakov and K. A. Ter-Martirosian, *Sov. Phys. JETP*, 648 (1957).